Decreasing the bandwidth of linear and nonlinear Thomson scattering radiation for electron bunches with a finite energy spread

Marcel Ruijter,[1,2] Vittoria Petrillo,[2,3] and Matt Zepf[4]

[1]*INFN, Sezione di Roma and Dipartimento di Fisica, University of Rome "La Sapienza", Piazzale Aldo Moro 5, 00185 Rome, Italy*
[2]*INFN-Sezione di Milano, via Celoria 16, 20133, Milano, Italy 2*
[3]*Università degli Studi di Milano, via Celoria 16, 2013, Italy 2*
[4]*Helmholtz Institute Jena, Fröbelstieg 3, 07743 Jena, Germany*

(Received 6 April 2020; accepted 8 February 2021; published 18 February 2021)

Relative narrow bandwidth-high energy radiation can be produced through Thomson scattering, where highly relativistic electrons collide with a laser pulse. The bandwidth of such a source is determined, among others factors, by the bandwidth of the laser pulse and the energy spread of the electrons. Here we investigate how the bandwidth of such a source can be minimized, with a particular emphasis on electron bunches with a correlated energy spread of several percent, that are typical for plasma based accelerator schemes. We show that by introducing a chirp on the laser pulse it is possible to compensate the broadening effect due to the energy spread of the electrons, and obtain the same bandwidth as a quasi-monochromatic plane wave laser pulse colliding with a monoenergetic electron bunch. Ultimately, the bandwidth of a Thomson source is limited by the acceptance angle and the initial transverse momentum of electrons (emittance).

DOI: 10.1103/PhysRevAccelBeams.24.020702

I. INTRODUCTION

Thomson scattering is the process of converting photons from low to high energy through the collision with relativistic electrons. This is a widely used approach to generate x- or γ-rays for imaging [1–5], medical applications [6,7] and nuclear photonic experiments [8,9]. The attraction for such a source lies in its high power, large transverse coherence and good level of tunability [10–14]. The latter is due to the emitted radiation's dependency on the electron energy (γ) and the (laser) photon frequency $\omega_{l,0}$: $\omega \propto \frac{\gamma^2}{1+(a)^2+\gamma^2\vartheta^2}\omega_{l,0}$, where ϑ is the angle of the scattered photon and (a) is the magnitude of the laser pulse given in terms of the normalized vector potential ($a_0 = \frac{eA_0}{mc^2}$, where e and m are the charge and mass of the electron respectively and c is the speed of light). Experiments like nuclear resonance fluorescence [8], nuclear astrophysics, and vacuum birefringence [15] require photon energies on the MeV scale with few percent bandwidth and a high flux [16]. For such photon energies the electron energy needs to be in the GeV range ($\gamma \sim 10^3$). Such electron bunches can be delivered by radio frequency or plasma based acceleration with a normalized emittance of $\leq$1 mm mrad [17–20]. To satisfy the bandwidth requirement the following relation needs to be minimized, which is (for negligible recoil and $a_0 \ll 1$) given by [21]

$$\frac{\sigma_\omega}{\omega} \cong \sqrt{\left(\Theta + \frac{\sigma_\epsilon}{\sigma_{W_{\text{bunch}}}}\right)^2 + \left(2\frac{\sigma_\gamma}{\gamma}\right)^2 + \left(\frac{\sigma_{\omega_l}}{\omega_l}\right)^2}, \quad (1)$$

where Θ is related to the acceptance angle $\vartheta_{\max}$ and is given by $\Theta = \frac{1}{\sqrt{12}}\frac{(\gamma\vartheta_{\max})^2}{1+(\gamma\vartheta_{\max})^2/2}$, σ_ϵ is rms normalized the emittance of the electron bunch, $\sigma_{W_{\text{bunch}}}$ is the rms bunch size in the transverse direction, σ_γ is the rms energy spread of the electron bunch and σ_{ω_l} is the bandwidth of the laser pulse. Even under otherwise ideal conditions, achieving a narrow Thomson-bandwidth requires that the acceptance angle is a fraction of the emission cone. In fact the leading term in Eq. (1) with the already given electron parameters requires $\vartheta_{\max} \sim \frac{1}{10\gamma}$. Radio frequency accelerators can provide electron bunches with very narrow energy spread (on the order of $<10^{-3}$) and can be used for low bandwidth Thomson sources, but they come at the cost of large (and expensive) facilities. On the other hand, plasma based acceleration schemes are short, cheap, and can deliver electron bunches with a charge on the order of ~100 pC, but with the downside that the energy spread is relatively large: few to tens of percent [17–19]. For a collision with a quasimonochromatic laser pulse these electron bunches are not

suitable. However, since the frequency of the Thomson scattered radiation depends linearly on the instantaneous frequency of the laser, an approach where the Thomson bandwidth is minimized by keeping $\gamma(t)^2\omega_l(t)$ constant is clearly attractive. Various studies have put forward a frequency modulation on the laser pulse to compensate for the nonlinear broadening of monochromatic electron bunches [22–25] and beam shape effects [26,27] (i.e., $\frac{1}{1+(a)^2}\omega_l = \text{const}$). A previous study [28] reported a method to compensate a correlated energy spread of an electron bunch by keeping the quantity $\frac{\gamma^2}{1+(a)^2}$ constant. Their method requires a laser intensity such that $1+a_0^2$ is substantially larger than 1 and a collision angle that allows electrons with different energy to be matched to the corresponding laser intensity along their interaction path. Furthermore, a laser pulse has a symmetric shape, which means a matched electron bunch needs a symmetric energy spread as well. In contrast, this work focuses on a method to use frequency modulation of the laser pulse to reduce the bandwidth of a Thomson source due to the energy spread of electrons, a method similar to the transverse gradient undulator [29–31]. Here, two interaction geometries of chirped laser pulses interacting with electron beams with a correlated energy spread are investigated, and we demonstrate that the ideal plane wave, zero electron energy spread performance can be retrieved.

II. ANALYTICAL DERIVATION OF THE REQUIRED LASER CHIRP

For the linear- (LT) [32,33] and nonlinear Thomson (NLT) [34,35] regime the emitted radiation can be calculated by the double differential equation [32]

$$\frac{d^2I}{d\omega d\Omega} = \frac{e^2}{4\pi^2 c}\left|\omega\sum_{i=0}^{N_e}\int_{-\infty}^{\infty} dt\,\hat{n}\times\hat{n}\times\vec{\beta}_i \exp\left[i\frac{\omega}{c}(ct-\hat{n}\cdot\vec{r}_i)\right]\right|^2, \tag{2}$$

where $d\Omega$ is the unit solid angle, ω is the emitted frequency, $\hat{n}$ the unit vector from the source to the detector in the far field, $\vec{\beta}_i$ and $\vec{r}_i$ are the velocity and trajectory of the ith particle. The number of emitted photons is then calculated by

$$N_{\text{ph}} = \int d\Omega \int d\omega \frac{1}{\hbar\omega}\frac{d^2I}{d\Omega d\omega}, \tag{3}$$

where $\hbar$ is the (modified) Planck constant. The equation of motion for an electron in an electromagnetic field is given by the Lorentz force (LF) [32]

$$\frac{dU^\mu}{ds} = -\frac{e}{mc^2}F^{\mu\nu}(X^\alpha)U_\nu = -(\partial^\mu a^\nu - \partial^\nu a^\mu)U_\nu, \tag{4}$$

where $ds = \frac{dct}{\gamma}$ is the interval, γ is the Lorentz factor of the particle, $U^\mu = \gamma(\frac{1}{\vec{\beta}}) \equiv \frac{dX^\mu}{ds}$ is the four velocity normalized to the speed of light, $F^{\mu\nu}$ is the electromagnetic field tensor and $a^\mu = \frac{e}{mc^2}A^\mu$ is the normalized vector potential. A circularly polarized laser pulse is described by

$$a^\mu = a_0\begin{pmatrix}0\\ \cos(\eta)\\ -\sin(\eta)\\ 0\end{pmatrix}\Psi(\vec{r})\mathcal{E}(\zeta), \tag{5}$$

where a_0 is the amplitude, η the phase of the laser pulse that can contain a frequency modulation, $\zeta = K_\mu X^\mu = \frac{\omega_{l,0}}{c}(ct-z)$ is the laser phase without chirp, the function $\Psi(\vec{r})$ describes the transverse profile and $\mathcal{E}(\zeta)$ describes the longitudinal profile of the laser pulse. A linearly polarized pulse is described by setting either $a^1 = 0$ or $a^2 = 0$. The motion of a single electron colliding head-on with a quasimonochromatic plane wave (PW) [Eq. (5) with $\Psi(\vec{r}) = 1$] is given by [24,36–38]

$$U^\mu = \begin{pmatrix}\gamma + \frac{(a)^2}{2}\gamma(1-\beta)\\ a^1\\ a^2\\ -\gamma\beta + \frac{(a)^2}{2}\gamma(1-\beta)\end{pmatrix}. \tag{6}$$

It has been demonstrated that the integral of Eq. (2) can be solved using the stationary phase approximation (SPA), i.e., find the points where the change of the is zero [24,39]. Previous studies ([24,39]) have shown that the integral of Eq. (2) can be solved using the stationary phase approximation (SPA), i.e., find the points where the change of the phase of Eq. (2) is zero. For backscattered radiation, the SPA condition is found by combining the oscillating function from the velocity component ($\vec{\beta}$) with the exponential in Eq. (2).

$$\begin{aligned}&\frac{d}{ds}\left(-\eta + \frac{\omega}{c}(ct+z)\right) = 0\\ &-\frac{\partial\eta}{\partial\zeta}\frac{d\zeta}{ds} + \frac{\omega}{c}(U^0+U^3) = 0,\end{aligned} \tag{7}$$

where the relations $\frac{d\zeta}{ds} = \frac{\omega_{l,0}}{c}\gamma(1+\beta)$ and $U^0+U^3 = \frac{1+(a)^2}{\gamma(1+\beta)}$ have been used (that can be obtained from solving the equation of motion [24,38]). If there is no chirp, i.e., $\eta = \zeta$, one finds the well-known formula for the emitted frequencies $\frac{\omega}{c} = \frac{\omega_{l,0}}{c}\frac{\gamma^2(1+\beta)^2}{1+(a)^2}$. For multiple particles, Eq. (7) can be generalized by substituting γ with the particle energy distribution. A correlated energy spread on the electrons

can be compensated by introducing a chirp on the laser pulse through the following relation

$$\frac{\omega}{c} = \text{const} = \frac{\omega_{l,0}}{c}\langle\gamma\rangle^2(1+\beta)^2 = \frac{\partial\eta(X)}{\partial\zeta}\frac{\gamma^2(X)(1+\beta)^2}{1+(a)^2}, \quad (8)$$

$$\frac{d\eta(X)}{d\zeta} \equiv \frac{\omega_l(X)}{c} = \frac{\omega_{l,0}}{c}\left(\frac{\langle\gamma\rangle}{\gamma(X)}\right)^2(1+(a)^2), \quad (9)$$

where X is the spatial coordinate of the energy spread of the electrons. Before solving for η, the effect on the emitted frequencies is further investigated. We restrict ourselves to only a linear chirp i.e., $\omega_l(X) = A + BX$. For a linearized chirp the required frequency spread ($\Delta\omega_B$) for $a_0 \ll 1$ is given by

$$\Delta\omega_B = \omega_{l,0}\left[\left(\frac{\langle\gamma\rangle}{\gamma_{\max}}\right)^2 - \left(\frac{\langle\gamma\rangle}{\gamma_{\min}}\right)^2\right]. \quad (10)$$

For an electron bunch of $\langle\gamma\rangle = 10^3$ and an energy spread of $\frac{\Delta\gamma}{\langle\gamma\rangle} = 0.05$, the relative frequency spread $\frac{\Delta\omega_B}{\omega_{l,0}} = 0.14$, which on the order of the bandwidth of high intensity lasers [e.g., Helmholtz Institute Jena JETI $\frac{\Delta\omega_l}{\omega_{l,0}} = 0.05$ [40] and LBNL Bella PW $\frac{\Delta\omega_l}{\omega_{l,0}} = 0.14$ [41] (values converted from FWHM to total difference)].

The contribution to the bandwidth of the emitted radiation for an energy spread of $\frac{\Delta\gamma}{\langle\gamma\rangle} = 0.05$ is $2\frac{\sigma_\gamma}{\gamma} \approx 0.0166$. To have $\frac{\sigma_{\omega_l}}{\omega_{l,0}} < 2\frac{\sigma_\gamma}{\gamma}$, we find that the minimum pulse length in number of wavelengths is $N_c > 60$ (taken that the bandwidth of a quasimonochromatic laser, i.e., the Fourier limited bandwidth, scales as $\frac{\sigma_{\omega_l}}{\omega_{l,0}} \propto \frac{1}{N_c}$ [42]).

Figure 1 (right) shows that the radiation bandwidth for a PW laser pulse of $N_c = 30$ and monoenergetic electrons is approximately equal to the case for a pulse of length $N_c = 150$ and an electron energy spread of $\frac{\Delta\gamma}{\langle\gamma\rangle} = 0.05$. This can be seen in Fig. 1 (right) which shows that the bandwidth of the emitted spectrum for a PW laser pulse length of $N_c = 30$ and no energy spread on the electrons has approximately the same bandwidth as that for a pulse length of $N_c = 150$ and an energy spread of $\frac{\Delta\gamma}{\langle\gamma\rangle} = 0.05$. Figure 1 (left) shows two simulations with different number of electrons, and we conclude that $N_e = 10^3$ has sufficient accuracy for the purpose of this study. The longitudinal profile of the PW is chosen to be

$$\mathcal{E}(\zeta) = \text{sech}\left(\frac{\zeta\sqrt{2}}{N_c}\right). \quad (11)$$

We consider two different geometries to compensate the increased Thomson-bandwidth due to the finite energy spread: transversely (TC) and longitudinally (LC) chirped. Figure 2 shows a sketch of both cases. To make a direct comparison between the two schemes the interaction length (i.e., the distance an electron propagates through the laser field) is set to $L_I = \frac{2\pi N_c}{\frac{\omega_{l,0}}{c}}$ (with larger L_I reducing the laser's contribution to the bandwidth).

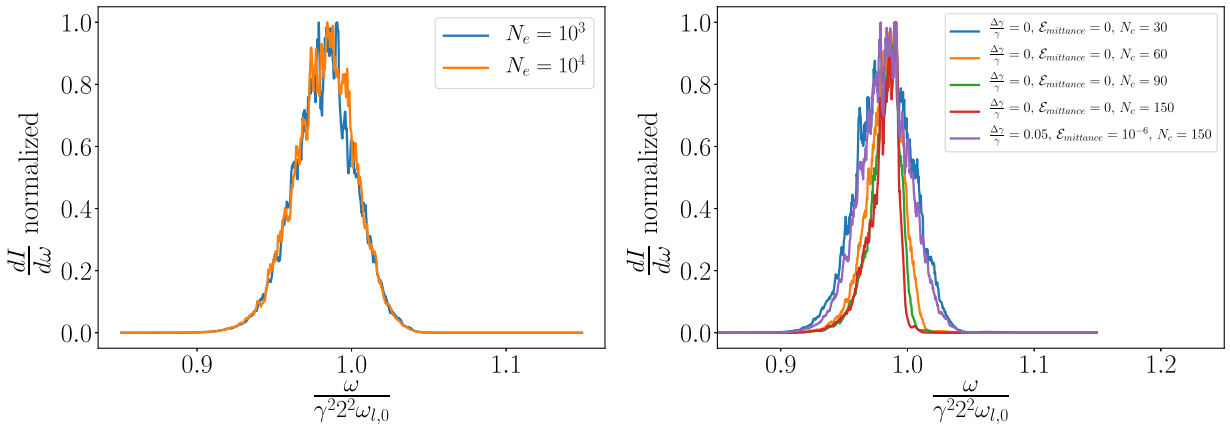

FIG. 1. Calculated spectra ($\frac{dI}{d\omega}$) within $\vartheta_{\max} = \frac{1}{10\gamma}$ for a circularly polarized PW laser pulse with parameters $a_0 = 10^{-1}$, $\omega_{l,0} = 1.77 \times 10^{15}$ [$\frac{1}{s}$] and electron parameters $\sigma_{x,y} = 15 \times 10^{-4}$ [cm], $\sigma_z = 15.75 \times 10^{-4}$ [cm], $\gamma = 10^3$. Left: spectra as function of the number of macro particles (N_e) with $\frac{\Delta\gamma}{\gamma} = 0.05$ and $\mathcal{E}_{\text{mittance}} = 10^{-6}$ [mm mrad]. From the results we conclude that $N_e = 10^3$ has sufficient accuracy for the purpose of this study. Right: spectra as function of N_c and an ideal electron bunch: $\frac{\Delta\gamma}{\gamma} = 0$ and $\mathcal{E}_{\text{mittance}} = 0$ [mm mrad]. It also includes a realistic electron bunch with $\frac{\Delta\gamma}{\gamma} = 0.05$ and $\mathcal{E}_{\text{mittance}} = 10^{-6}$ [mm mrad] for the PW $N_c = 150$ case (purple). The bandwidth of the emitted radiation for $N_c = 30$ and an ideal electron bunch roughly equals that of $N_c = 150$ and realistic one.

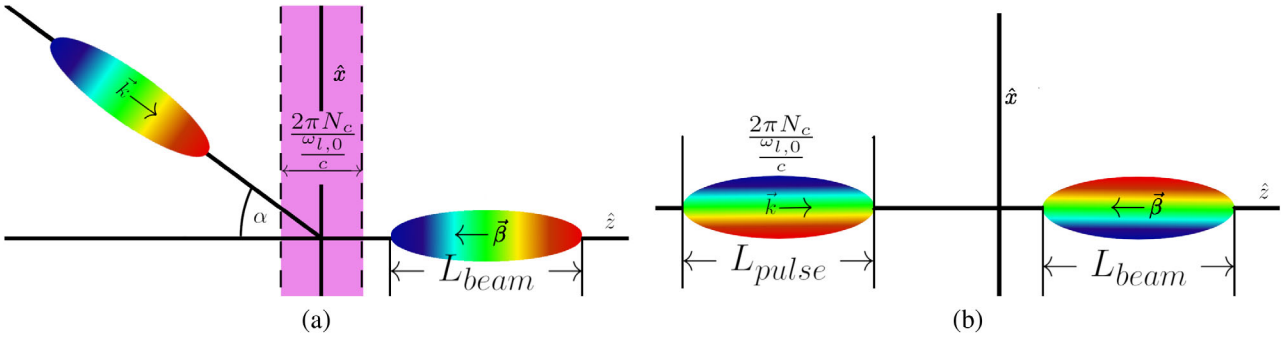

FIG. 2. Schematic of the two possible geometries for a chirped laser pulse. (a) Longitudinally chirped laser pulse. The shaded area indicates the interaction length (L_I). The model for the chirp is set up such that a pulse that travels along the z-axis and is rotated by an angle α. (b) Transversely chirped laser pulse. Here the length of the interaction is the length of the laser pulse after imposing a spatial chirp.

III. TRANSVERSE CHIRP

In this model, an electron bunch with a correlated energy spread in the transverse direction ($\hat{x}$) collides head-on with a spatially chirped laser pulse. The condition for the chirp is

$$\frac{d\eta}{d\zeta} \equiv \frac{\omega_l(x)}{c} = A + Bx = \left(\frac{\langle\gamma\rangle}{\gamma(x)}\right)^2 \frac{\omega_{l,0}}{c}, \tag{12}$$

$$\eta = \frac{\omega_l(x)}{c}\zeta. \tag{13}$$

The stability of this kind of chirping depends on the trajectory of an electron during the laser pulse interaction and the initial transverse momentum of the electron bunch or the collision angle between the electron bunch and laser pulse. The total required bandwidth is given by

$$\begin{aligned}\Delta\omega_B &= \omega_l(x=0) - \omega_l(x = W_{\text{bunch}}) \\ &= \omega_{l,0}\left[\left(\frac{\langle\gamma\rangle}{\gamma(0)}\right)^2 - \left(\frac{\langle\gamma\rangle}{\gamma(W_{\text{bunch}})}\right)^2\right],\end{aligned} \tag{14}$$

where W_{bunch} is the width of the electron bunch. The transverse motion of the electron during the laser pulse scales with $\frac{a_0}{\gamma(1+\beta)\frac{\omega_{l,0}}{c}}$ (integration of Eq. (6) using the slowly varying amplitude approximation). Thus the range of frequencies that a single electron experiences when colliding head-on is given by

$$\frac{\Delta\omega_\gamma}{\omega_{l,0}} = \left[\left(\frac{\langle\gamma\rangle}{\gamma_{\text{top}}}\right)^2 - \left(\frac{\langle\gamma\rangle}{\gamma_{\text{bottom}}}\right)^2\right] \frac{a_0}{\frac{\omega_{l,0}}{c}\langle\gamma\rangle(1+\beta)} \frac{}{W_{\text{bunch}}}. \tag{15}$$

In general, $W_{\text{bunch}} \gg \frac{a_0}{\frac{\omega_{l,0}}{c}\langle\gamma\rangle(1+\beta)}$ and therefore the change of frequency for a head-on collision is negligible. One must be careful with increasing W_{bunch} while keeping the width of the laser W_0 constant, since different parts of the electron bunch will experience a different value of a_0 if $\Psi(\vec{r})$ has a large transverse gradient. An electron colliding under an angle α_ϵ (whether due to an angle between the bunch and the laser pulse or due to divergence/emittance) gives a contribution of

$$\begin{aligned}\Delta\omega_\epsilon &= \omega_l(ct_1, x_1) - \omega_l(ct_0, x_0) \\ &= \left[\left(\frac{\langle\gamma\rangle}{\gamma_{\text{top}}}\right)^2 - \left(\frac{\langle\gamma\rangle}{\gamma_{\text{bottom}}}\right)^2\right] \frac{L_I}{W_{\text{bunch}}} \frac{\beta_x}{\beta_z},\end{aligned} \tag{16}$$

where $a_0 \ll 1$ so that $\tan(\alpha_\epsilon) = \frac{\Delta x}{L_I} = \frac{\beta_x}{\beta_z}$. For an electron bunch it can be generalized to the product of its energy spread and divergence.

In [22–25] it is shown that a laser pulse with $a0 > 1$ makes a significant contribution to the overall Thomson bandwidth, but can be compensated using a chirp along the propagation direction of the laser pulse. It is in principle possible to combine the chirp that compensates the energy spread of the electrons with one that compensates for the non-linear broadening, because they are along different axes:

$$\frac{\partial\eta}{\partial\zeta} = \frac{\omega_l(x)}{c}\frac{\omega_l(\zeta)}{c} = \frac{\omega_{l,0}}{c}\left(\frac{\langle\gamma\rangle}{\gamma(x)}\right)^2(1 + [a(\zeta)]^2), \tag{17}$$

The choice for the laser pulse's shape for the TC case is

$$\Psi(\vec{r}) = \frac{q(0)}{q(z)}\exp\left[-i\frac{\omega_{l,0}}{c}\frac{x^2+y^2}{2q(z)}\right], \tag{18}$$

$$\mathcal{E}(\zeta) = \text{sech}\left(\frac{\zeta\sqrt{2}}{N_c}\right) \tag{19}$$

Fig. 3 shows simulation results for the linear ($a_0 = 0.1$) and non-linear ($a_0 = 1$) TC where the electrons have an energy of $\langle\gamma\rangle = 10^3$ and $\frac{\Delta\gamma}{\gamma} = 0.05$ and no initial transverse momentum.

For TC with $a_0 < 1$ the bandwidth scales as

$$\frac{\sigma_{\omega,TC}}{\omega} = \sqrt{\left(\Theta + \frac{\sigma_\epsilon}{\sigma_{W_{\text{bunch}}}}\right)^2 + \left(\frac{\Delta\omega_{\gamma,\epsilon}}{6\omega_{l,0}}\right)^2_{TC} + \left(\frac{\sigma_{\omega_l}}{\omega_{l,0}}\right)^2}, \tag{20}$$

where $\Delta\omega_{\gamma,\epsilon}$ is given by Eq. (16).

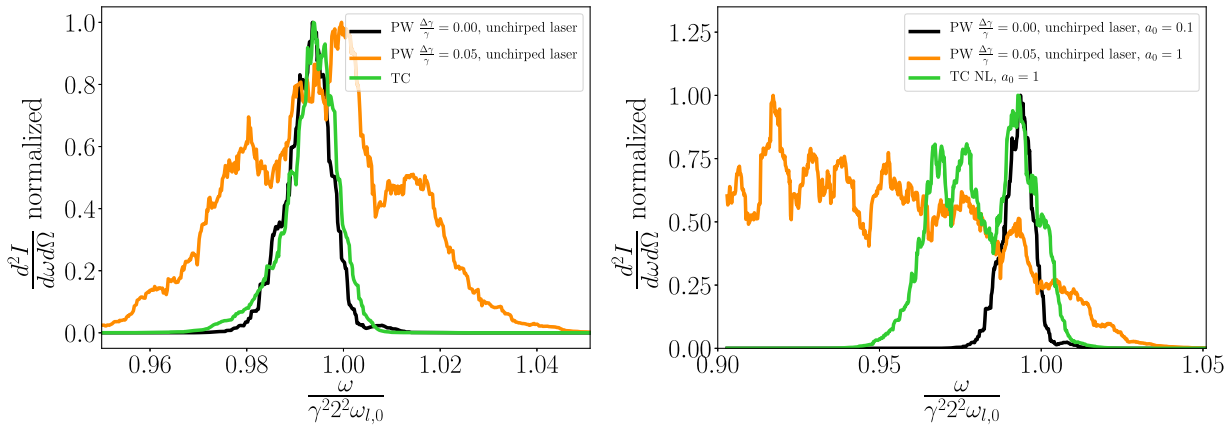

FIG. 3. Calculated on-axis spectra for a circularly polarized laser pulse with parameters $\omega_{l,0}=1.77\times10^{15}$ $[\frac{1}{s}]$, $N_c=150$, $W_0=300\times10^{-4}$ [cm], and electron parameters $N_e=10^3$, $\sigma_{x,y}=15\times10^{-4}$ [cm], $\sigma_z=15.75\times10^{-4}$ [cm], $\gamma=10^3$ where the energy spread is linear in the $\hat{x}$ direction with a magnitude $\frac{\Delta\gamma}{\gamma}=0.05$ and the electrons do not have initial transverse momentum. Left: laser intensity of $a_0=10^{-1}$. The PW monoenergetic electron bunch case is reproduced when using a chirped laser pulse as given by Eq. (13). Right: $a_0=1$ and the chirp of the laser pulse given by Eq. (17).

IV. LONGITUDINAL CHIRP

In a head-on collision of an electron and longitudinally chirped laser pulse, the electron will experience all the frequencies contained within the laser pulse. This would result in a broadened spectrum according to Eq. (7). However, the electron will travel only through a part of the laser part and thus only experience a fraction of the frequencies when colliding under an incident angle (α). To cancel the transverse component of the laser pulse's momentum a second laser pulse is added to the system colliding under $-\alpha$, i.e., within the interaction region (on axis) the electron will experience a fraction of the laser pulses traveling only in $\hat{z}$. The fraction of the laser pulse containing the frequency matched to an electron's energy is $\mathcal{L}=\frac{\beta}{1+\beta}L_I$, because the electron and laser pulse counter propagate. More plainly: the chirp needs to be stretched by $\mathcal{L}$. The chirp condition is then found to be

$$\frac{\partial\eta}{\partial\zeta}\equiv\frac{\omega_l(\zeta)}{c}=A+B\zeta=\frac{\omega_{l,0}}{c}\left(\frac{\langle\gamma\rangle}{\gamma(\frac{1+\beta}{\beta}z)}\right)^2. \tag{21}$$

The frequencies experienced by a single electron is then given by the end points of the interaction region:

$$\begin{aligned}\Delta\omega_{\gamma,\epsilon}&=\omega_l\left(ct=0,-\frac{L_I}{2}\right)-\omega_l\left(ct=ct_1,z=\frac{L_I}{2}\right)\\&=B(ct_1+L_I).\end{aligned} \tag{22}$$

If $a_0\ll1$, ct_1 can be approximated by $\frac{L_I}{\beta\cos(\alpha_\epsilon)}$, where $\tan(\alpha_\epsilon)=\frac{\beta_x}{\beta_z}$. Solving (22) gives

$$\frac{\Delta\omega_{\gamma,\epsilon}}{\omega_{l,0}}=\left(\left(\frac{\langle\gamma\rangle}{\gamma_{\text{front}}}\right)^2-\left(\frac{\langle\gamma\rangle}{\gamma_{\text{rear}}}\right)^2\right)\frac{1+\beta\cos(\alpha_\epsilon)}{\beta\cos(\alpha_\epsilon)}\frac{1}{L_{\text{rat}}}, \tag{23}$$

where $L_{\text{rat}}=\frac{L_{\text{bunch}}}{L_I}$ and α_ϵ is the incident angle of the electron (i.e., the electron has a transverse momentum). The difference of $\Delta\omega_{\gamma,\epsilon}$ between $\alpha_\epsilon=10$ deg and $\alpha_\epsilon=0$ for an electron with $\gamma=10^3$ and $\frac{\Delta\gamma}{\gamma}=0.05$ is on the order of 10^{-3} and therefore for the remainder of this paper $\alpha_\epsilon=0$. To obtain a narrow bandwidth $\Delta\omega_{\gamma,\epsilon}$ needs to be near zero.

When $\frac{\Delta\omega_{\gamma,\epsilon}}{\omega_{l,0}}\ll1$ Eq. (21) can be solved using the slowly varying amplitude approximation. This results in

$$\eta=\frac{\omega_l(\zeta)}{c}\zeta. \tag{24}$$

A chirp for the nonlinear broadening [22–24,43] cannot be used in this scheme, since the chirp for energy compensation is along ζ and the condition of $\frac{\Delta\omega_{\gamma,\epsilon}}{\omega_{l,0}}\ll1$ would be violated. For the calculation of the spectrum the laser pulse is described by two Gaussian beams crossing each other in the origin. The combined field results in a PW wave along the z axis where Eq. (21) is valid. The choice for the laser pulse's shape for the LC case is

$$\zeta=\frac{\omega_{l,0}}{c}(ct-z'), \tag{25}$$

$$\eta=\frac{\omega_l(\zeta)}{c}\zeta, \tag{26}$$

$$x'(\alpha)=z\sin(\alpha)+x\cos(\alpha), \tag{27}$$

$$z'(\alpha)=z\cos(\alpha)-x\sin(\alpha), \tag{28}$$

$$\Psi(\vec{r})=\frac{G(r[\alpha])+G[r(-\alpha)]}{2}, \tag{29}$$

$$G(r(\alpha)) = \frac{q(0)}{q(z')}\exp\left[-i\frac{\omega_{l,0}}{c}\frac{x'^2+y^2}{2q(z')}\right], \tag{30}$$

$$q(z) = q_0 + z, \tag{31}$$

$$q_0 = i\frac{W_0^2\frac{\omega_{l,0}}{c}}{2}, \tag{32}$$

$$\mathcal{E}(K_\mu X^\mu) = 1. \tag{33}$$

To keep the L_I and W_0 equal to the PW and TC case, the following relation is used for the angle of incidence:

$$\alpha = \sin^{-1}\left(\frac{2(\frac{3}{\sqrt{2}}W_0)}{L_I}\right). \tag{34}$$

Figure 4 shows the possible incident angles and the final configuration of this scheme.

In Fig. 5, the results from simulations are shown with the laser parameters $a_0 = 10^{-1}$, $N_c = 150$, $W_0 = 30\times10^{-4}$ [cm] and $\alpha = 52.8$ deg and electron parameters $\langle\gamma\rangle = 10^3$, with an energy spread linear in $\hat{z}$ and no initial transverse momentum. For lower a_0 and lower $\langle\gamma\rangle$ similar results are found. The bandwidth of the emitted radiation is predicted by Eq. (22) and approaches the limit of the PW with a monochromatic electron bunch.

The bandwidth for the LC case scales as

$$\frac{\sigma_{\omega,LC}}{\omega} = \sqrt{\left(\Theta + \frac{\sigma_\epsilon}{\sigma_{W_{\text{bunch}}}}\right)^2 + \left(\frac{\Delta\omega_{\gamma,\epsilon}}{6\omega_{l,0}}\right)^2_{LC} + \left(\frac{\sigma_{\omega_{l,0}}}{\omega_{l,0}}\right)^2}, \tag{35}$$

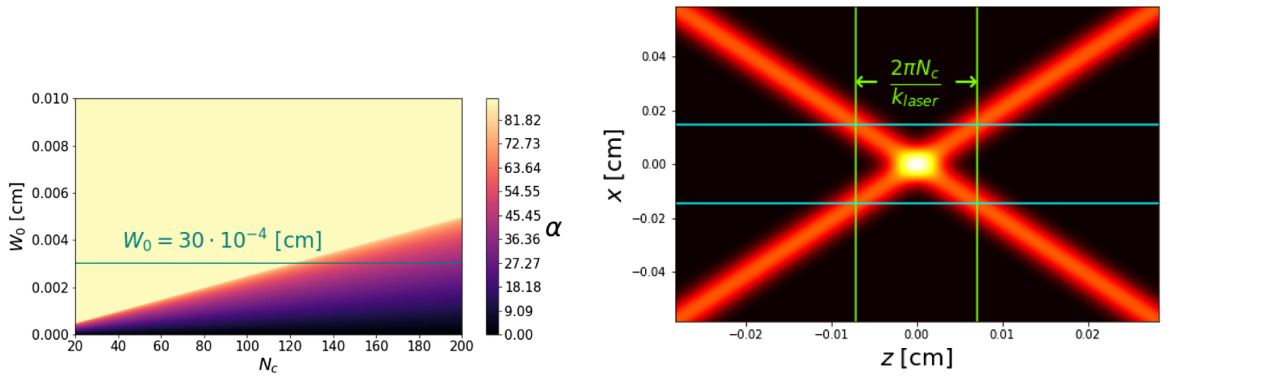

(a) (b)

FIG. 4. Possible configuration for LC with $\omega_{l,0} = 1.77\times10^{15}$ [$\frac{1}{s}$] (a) Shows the possible angles as function of N_c (proportional to the interaction length). The blue line indicates the width $W_0 = 30\times10^{-4}$ [cm]. The yellow shaded region indicates incompatible sets of parameters.(b) Intensity profile of the two Gaussian beams in the x and z plane.

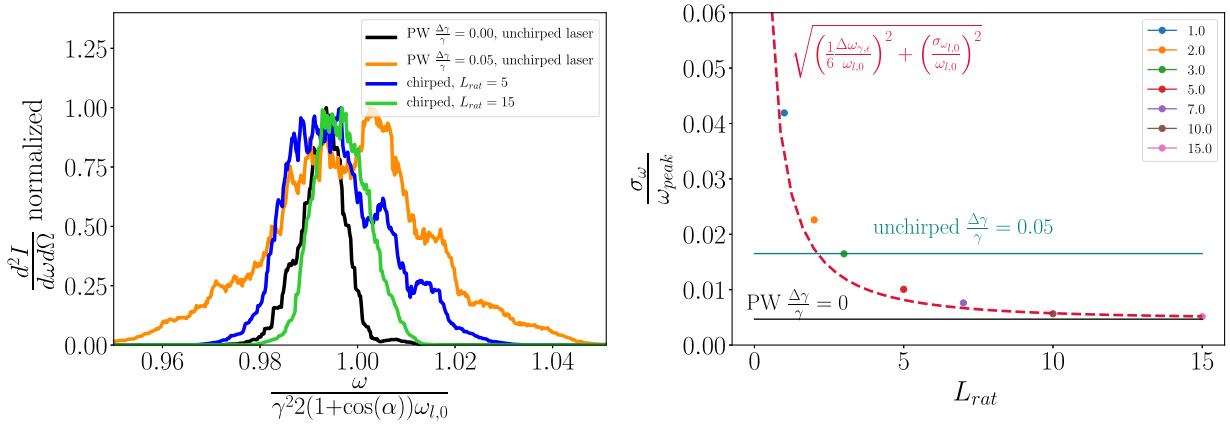

FIG. 5. Calculated on-axis spectra for a circularly polarized laser pulse with $\omega_{l,0} = 1.77\times10^{15}$ [$\frac{1}{s}$] parameters, $a_0 = 10^{-1}$, $N_c = 150$, $W_0 = 30\times10^{-4}$ [cm] and $\alpha = 52.8$ deg, and electron parameters $N_e = 10^3$, $\sigma_{x,y} = 15\times10^{-4}$ [cm], $\sigma_z = 15.75\times10^{-4}$ [cm], $\langle\gamma\rangle = 10^3$, with an energy spread $\frac{\Delta\gamma}{\gamma} = 0.05$ linear in $\hat{z}$ and no initial transverse momentum. Left: spectra for the electrons colliding with two Gaussian beams. Right: the bandwidth of the emitted spectrum as function of L_{rat}. Equation (23) predicts accurately the bandwidth of the emitted spectrum. The factor of $\frac{1}{6}$ for $\frac{\Delta\omega_{\gamma,\epsilon}}{\omega_{l,0}}$ is for the conversion from full bandwidth to rms values. For the $\frac{\Delta\gamma}{\gamma} = 0.05$ the limit of Eq. (23) is visible, as the bandwidth of the emitted spectrum cannot be lower than the PW monoenergetic electron bunch case.

where $\frac{\sigma_{\omega_{l,0}}}{\omega_{l,0}}$ is the Fourier limited bandwidth of the laser field as the electron traverses it, $\Delta\omega_{\gamma,\epsilon}$ is given by Eq. (23) and the factor $\frac{1}{6}$ is used to get the rms value.

V. COMPARISON AND DISCUSSION

The radiation ($\frac{dI}{d\omega}$) and N_{ph} are calculated for four cases: quasimonochromatic PW laser pulse colliding with a monochromatic electron bunch (PW $\Delta\gamma = 0.00$, $\mathcal{E}_{\mathrm{mittance}} = 1$ [mm mrad]), quasimonochromatic PW laser pulse colliding with electron bunch with an energy spread (PW $\Delta\gamma = 0.05$, $\mathcal{E}_{\mathrm{mittance}} = 0$ [mm mrad]), longitudinally (LC) and transversely chirped (TC) laser pulse as described in the previous sections. For LC and TC, the emittance of the electron bunch is $\mathcal{E}_{\mathrm{mittance}} = 1$ [mm mrad]. For all cases, the number of macro particles in the simulation are $N_e = 10^3$ and for the N_{ph} the charge of the electron bunch is 1×10^{-9} [C]. The spectra for a circularly polarized laser pulse are shown in Fig. 6 and the energies of the laser pulses, emitted radiation and the bandwidth are provided in Table I. The bandwidth reduction is similar for a linearly polarized laser pulse, as can be see in Fig. 7.

Figures 6 and 7 and Table I show that the bandwidth of a monochromatic laser pulse colliding with a monoenergetic electron bunch can be recovered with the described method of using a linearly chirped laser pulse colliding with an electron bunch with a correlated energy spread. The method requires a frequency range for the laser pulse equal to $2\frac{\Delta\gamma}{\gamma}$. This is on the same order as the bandwidth of high intensity lasers for $\gamma = 10^3$ with a 5% energy spread. The presented methods still work rather well even for a mismatch between the chirp and the electron energy spread (red curves in Figs. 6).

For TC not only the PW bandwidth can be recovered but also N_{ph} is roughly the same. For this geometry the electron bunch distribution could be obtained by a simple device like a dipole magnet. Additionally, the TC can also be expanded into the NLT regime. In case there is a transverse misalignment between the laser pulse and the electron bunch, the peak of the emitted frequency would shift.

LC has a reduced N_{ph} that can be attributed to the interference of the two laser pulses, i.e., an electron traveling off axis along the $-\hat{z}$ axis does not experience a longitudinal Gaussian profile. A disadvantage that is shared with the method by [28] is that each electron only sees a slice of the laser pulse. This means that the ratio of emitted photons per laser photons is less than that of a head-on collision. Within the L_I, only a "single" frequency and electron energy can be present, thus requiring the laser pulse and electron bunch to be rather long $L_{\mathrm{pulse}} \geq L_{\mathrm{rat}} L_I$.

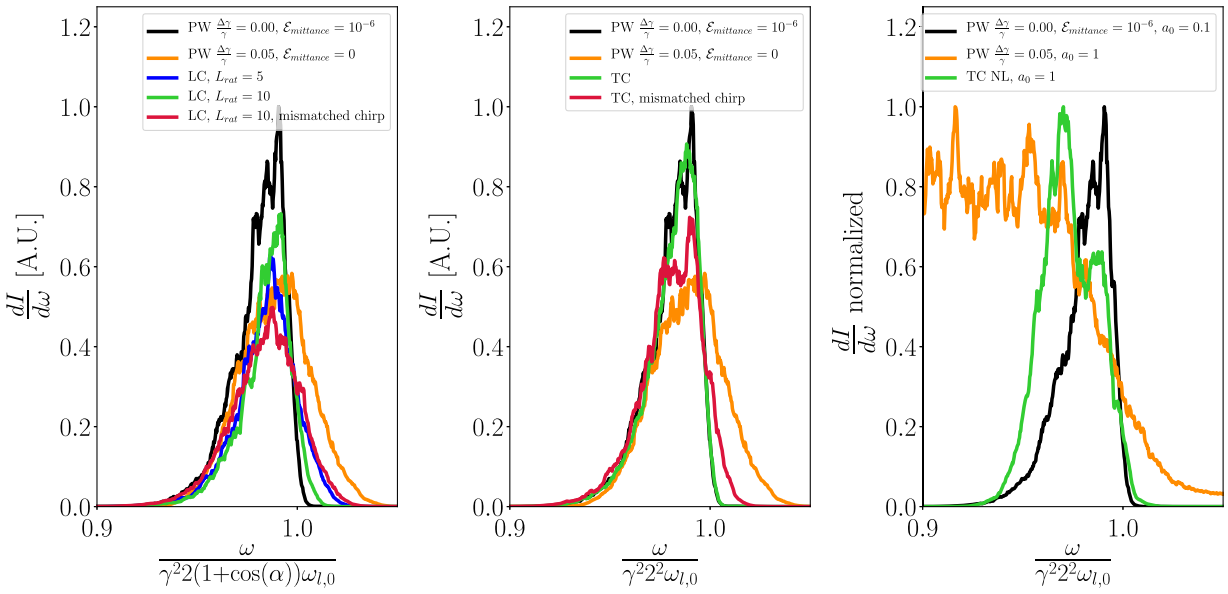

FIG. 6. Calculated spectra within $\vartheta_{\max} = \frac{1}{10\gamma}$ for a circularly polarized laser pulse with parameters $\omega_{l,0} = 1.77 \times 10^{15}$ [$\frac{1}{s}$], $N_c = 150$, $W_0 = 30 \times 10^{-4}$ [cm], and electron parameters $\gamma = 10^3$, $\sigma_{x,y} = 15 \times 10^{-4}$ [cm] and $\sigma_z = 15.75 \times 10^{-4}$ [cm]. Further specific parameters are given below. For the PW case two simulations were performed: one with $\frac{\Delta\gamma}{\gamma} = 0.00$ and $\mathcal{E}_{\mathrm{mittance}} = 1$ [mm mrad] and one with $\frac{\Delta\gamma}{\gamma} = 0.05$ and $\mathcal{E}_{\mathrm{mittance}} = 0$ [mm mrad]. Left: LC with collision angle $\alpha = 52.8$ deg and $a_0 = 0.1$. The frequency bandwidth for cases in blue, green and red is $\frac{\Delta\omega_B}{\omega_{l,0}} = 0.14$. The energy spread for the electron bunch for blue and green is $\frac{\Delta\gamma}{\gamma} = 0.05$ and for red $\frac{\Delta\gamma}{\gamma} = 0.07$. The peak frequency is lower due to the collision angle. Middle: TC with $a_0 = 0.1$. For the frequency bandwidth for cases in green and red is $\frac{\Delta\omega_B}{\omega_{l,0}} = 0.14$. The energy spread for the electron bunch for green is $\frac{\Delta\gamma}{\gamma} = 0.05$ and for red $\frac{\Delta\gamma}{\gamma} = 0.07$. Right: TC NL with $a_0 = 1$. The vertical axis is normalized to 1. This is done because the unchirped laser pulse case has very little radiation in this region, and to compare it to the LT PW case which has a different amplitude.

TABLE I. Parameters of Fig. 6 with the same color code: Energy of the laser pulse, the energy spread of the electrons, the chirp coefficients as described in Eq. (13) and (21), the laser strength parameter of the pulse, the peak frequency, bandwidth and number of photons of the emitted radiation. These numbers are for a single laser pulse–electron bunch collision. For all the chirped cases a frequency bandwidth of $\frac{\Delta\omega_B}{\omega_{l,0}} = 0.14$ has been used.

	PW (black)	PW (orange)	LC, $L_{\text{rat}} = 5$ (blue)	LC, $L_{\text{rat}} = 10$ (green)	LC, $L_{\text{rat}} = 10$, mismatched chirp (red)
$\frac{\Delta\gamma}{\gamma}$	0.00	0.05	0.05	0.05	0.07
chirp coeff. A	…	…	1.00	1.00	1.00
chirp coeff. B	…	…	1.79×10^{-5}	5.98×10^{-6}	5.98×10^{-6}
E_{laser} [Joule]	0.14	0.14	0.52	1.06	1.06
a_0	0.1	0.1	0.1	0.1	0.1
$\langle\frac{\omega}{c}\rangle \frac{10^{11}}{\text{cm}}$	2.33	2.31	1.86	1.86	1.86
N_{ph}	0.90×10^6	0.94×10^6	0.69×10^6	0.66×10^6	0.70×10^6
$\frac{\sigma_\omega}{\omega}$ (rms)	0.013	0.018	0.015	0.013	0.017

	PW (black)	PW (orange)	TC (green)	TC, mismatched chirp (red)	TC NL (green)
$\frac{\Delta\gamma}{\gamma}$	0.00	0.05	0.05	0.07	0.05
E_{laser} [Joule]	0.14	0.14	0.16	0.16	13.6
a_0	0.1	0.1	0.1	0.1	1
$\langle\frac{\omega}{c}\rangle \frac{10^{11}}{\text{cm}}$	2.33	2.31	2.30	2.31	2.31
N_{ph}	0.90×10^6	0.94×10^6	0.88×10^6	0.89×10^6	5.5×10^7
$\frac{\sigma_\omega}{\omega}$ (rms)	0.013	0.018	0.013	0.015	0.015
chirp coeff. A	…	…	1.00	1.00	$(\hat{x})$ 1.00, $(\hat{\zeta})$-106
chirp coeff. B	…	…	8.97×10^{-6}	8.97×10^{-6}	$(\hat{x})$ 1.79×10^{-3}, $(\hat{\zeta})$ 1

A longitudinal misalignment would shift the peak frequency of the emitted radiation.

In this work only a linearly chirped laser pulse has been used, which limits the use to a linear energy spread distribution of electron. By using a higher order chirp, sometimes referred to as chromatic dispersion terms, the energy spread of the electrons can also take different distributions.

The bandwidth of a Thomson source can potentially be further minimized by decreasing the emittance of the

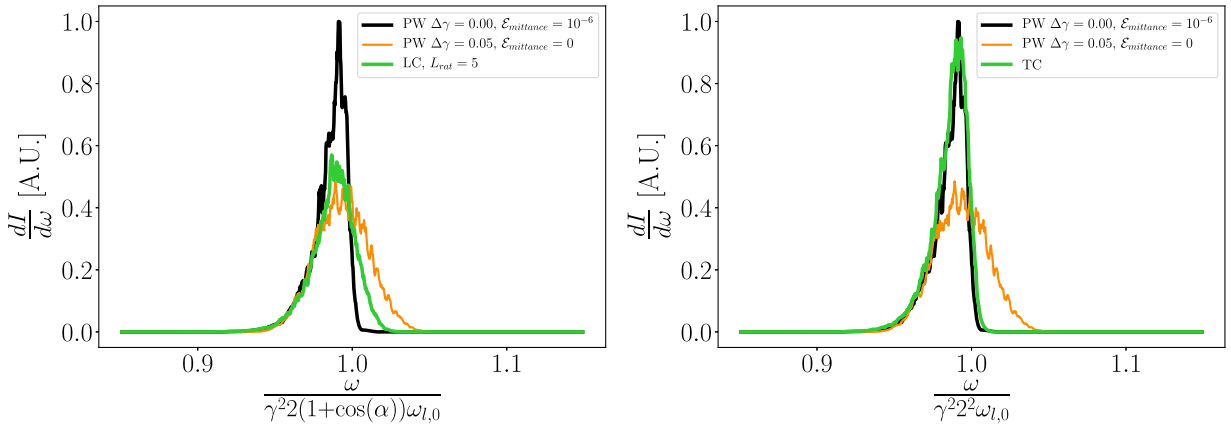

FIG. 7. Results from the calculation of $\frac{dI}{d\omega}$ for a linearly polarized laser pulse. Parameters of the calculations are $\vartheta_{\max} = \frac{1}{10\gamma}$, laser parameters $\omega_{l,0} = 1.77 \times 10^{15}$ $[\frac{1}{s}]$, $N_c = 150$, $W_0 = 30 \times 10^{-4}$ [cm], $a_0 = 0.1$, and electron parameters are $\gamma = 10^3$, $\sigma_{x,y} = 15 \times 10^{-4}$ [cm] and $\sigma_z = 15.75 \times 10^{-4}$ [cm]. Further specific parameters are given below. For the PW case two simulations were performed: one with $\frac{\Delta\gamma}{\gamma} = 0.00$ and $\mathcal{E}_{\text{mittance}} = 1$ [mm mrad] and one with $\frac{\Delta\gamma}{\gamma} = 0.05$ and $\mathcal{E}_{\text{mittance}} = 0$ [mm mrad]. The frequency bandwidth for cases in green is $\frac{\Delta\omega_B}{\omega_{l,0}} = 0.14$ for an energy spread of the electron bunch $\frac{\Delta\gamma}{\gamma} = 0.05$. Left: LC with collision angle $\alpha = 52.8$ deg and Right: TC.

electron bunch (σ_ϵ) and increasing the interaction length. Ultimately the Thomson bandwidth is limited by the acceptance angle $\vartheta_{\max}$. Reducing $\vartheta_{\max}$ further however also reduces N_{ph} and thus making the system less efficient.

In conclusion, we showed that a narrow bandwidth Thomson source is achievable for electron bunches with a finite energy spread by using a chirped laser pulse. This method would allow plasma based electron bunches to compete with traditional accelerator structures, because the energy spread of the electrons is negated.

[1] M. Bech, O. Bunk, C. David, R. Ruth, J. Rifkin, R. Loewen, R. Feidenhans'l, and F. Pfeiffer, Hard x-ray phase-contrast imaging with the Compact Light Source based on inverse Compton x-rays, J. Synchotron Radiat. **16**, 43 (2009).

[2] K. Achterhold, M. Bech, S. Schleede, G. Potdevin, R. Ruth, R. Loewen, and F. Pfeiffer, Monochromatic computed tomography with a compact laser-driven x-ray source, Sci. Rep. **3**, 1313 (2013).

[3] B. Golosio, M. Endrizzi, P. Oliva, P. Delogu, M. Carpinelli, I. Pogorelsky, and V. Yakimenko, Measurement of an inverse Compton scattering source local spectrum using k-edge filters, Appl. Phys. Lett. **100**, 164104 (2012).

[4] F. G. Meinel, F. Schwab, S. Schleede, M. Bech, J. Herzen, K. Achterhold, S. Auweter, F. Bamberg, A. Ö. Yildirim, A. Bohla *et al.*, Diagnosing and mapping pulmonary emphysema on x-ray projection images: Incremental value of grating-based x-ray dark-field imaging, PLoS One **8**, e59526 (2013).

[5] F. Schwab, S. Schleede, D. Hahn, M. Bech, J. Herzen, S. Auweter, F. Bamberg, K. Achterhold, A. Ö. Yildirim, A. Bohla *et al.*, Comparison of contrast-to-noise ratios of transmission and dark-field signal in grating-based x-ray imaging for healthy murine lung tissue, Z. Med. Phys. **23**, 236 (2013).

[6] K. J. Weeks, V. N. Litvinenko, and J. M. J. Madey, The Compton backscattering process and radiotherapy, Med. Phys. **24**, 417 (1997).

[7] T. Brümmer, A. Debus, R. Pausch, J. Osterhoff, and F. Grüner, Design study for a compact laser-driven source for medical x-ray fluorescence imaging, Phys. Rev. Accel. Beams **23**, 031601 (2020).

[8] B. J. Quiter, B. A. Ludewigt, V. V. Mozin, C. Wilson, and S. Korbly, Transmission nuclear resonance fluorescence measurements of 238u in thick targets, Nucl. Instrum. Methods Phys. Res., Sect. B **269**, 1130 (2011).

[9] A. Bacci *et al.*, Electron linac design to drive bright compton back-scattering gamma-ray sources, J. Appl. Phys. **113**, 194508 (2013).

[10] I. V. Pogorelsky, I. Ben-Zvi, T. Hirose, S. Kashiwagi, V. Yakimenko, K. Kusche, P. Siddons, J. Skaritka, T. Kumita, A. Tsunemi, T. Omori, J. Urakawa, M. Washio, K. Yokoya, T. Okugi, Y. Liu, P. He, and D. Cline, Demonstration of $8x10^18$ photons/second peaked at 1.8 Å in a relativistic Thomson scattering experiment, Phys. Rev. Accel. Beams **3**, 090702 (2000).

[11] W. J. Brown, S. G. Anderson, C. P. J. Barty, S. M. Betts, R. Booth, J. K. Crane, R. R. Cross, D. N. Fittinghoff, D. J. Gibson, F. V. Hartemann, E. P. Hartouni, J. Kuba, G. P. Le Sage, D. R. Slaughter, A. M. Tremaine, A. J. Wootton, P. T. Springer, and J. B. Rosenzweig, Experimental characterization of an ultrafast Thomson scattering x-ray source with three-dimensional time and frequency-domain analysis, Phys. Rev. Accel. Beams **7**, 060702 (2004).

[12] V. G. Nedorezov, A. A. Turinge, and Y. M. Shatunov, Photonuclear experiments with Compton-backscattered gamma beams, Phys. Uspekhi **47**, 341 (2004).

[13] M. Babzien, I. Ben-Zvi, K. Kusche, I. V. Pavlishin, I. V. Pogorelsky, D. P. Siddons, V. Yakimenko, D. Cline, F. Zhou, T. Hirose, Y. Kamiya, T. Kumita, T. Omori, J. Urakawa, and K. Yokoya, Observation of the Second Harmonic in Thomson Scattering from Relativistic Electrons, Phys. Rev. Lett. **96**, 054802 (2006).

[14] R. Kuroda, H. Toyokawa, M. Yasumoto, H. Ikeura-Sekiguchi, M. Koike, K. Yamada, T. Yanagida, T. Nakajyo, F Sakai, and K. Mori, Quasi-monochromatic hard x-ray source via laser Compton scattering and its application, Nucl. Instrum. Methods Phys Res., Sect. A **637**, S183 (2011).

[15] Y. Nakamiya and K. Homma, Probing vacuum birefringence under a high-intensity laser field with gamma-ray polarimetry at the gev scale, Phys. Rev. D **96**, 053002 (2017).

[16] C. R. Howell *et al.*, *International Workshop on Next Generation Gamma-Ray Source* 12 (2020) [arXiv:2012.10843].

[17] W. Leemans and E. Esarey, Laser-driven plasma-wave electron accelerators, Phys. Today **62**, No. 3, 44 (2009).

[18] R. Weingartner, S. Raith, A. Popp, S. Chou, J. Wenz, K. Khrennikov, M. Heigoldt, A. R. Maier, N. Kajumba, M. Fuchs, B. Zeitler, F. Krausz, S. Karsch, and F. Grüner, Ultralow emittance electron beams from a laser-wakefield accelerator, Phys. Rev. Accel. Beams **15**, 111302 (2012).

[19] E. Svystun, R. W. Assmann, U. Dorda, A. F. Pousa, T. Heinemann, B. Marchetti, A. M. de la Ossa, P. A. Walker, M. K. Weikum, and J. Zhu, Beam quality preservation studies in a laser-plasma accelerator with external injection for eupraxia, Nucl. Instrum. Methods Phys. Res., Sect. A **909**, 90 (2018).

[20] C. B. Schroeder, C. Benedetti, E. Esarey, M. Chen, and W. P. Leemans, Two-color ionization injection using a plasma beatwave accelerator, Nucl. Instrum. Methods Phys. Res., Sect. A **909**, 149 (2018).

[21] N. Ranjan, B. Terzić, G. A. Krafft, V. Petrillo, I. Drebot, and L. Serafini, Simulation of inverse Compton scattering and its implications on the scattered linewidth, Phys. Rev. Accel. Beams **21**, 030701 (2018).

[22] I. Ghebregziabher, B. A. Shadwick, and D. Umstadter, Spectral bandwidth reduction of Thomson scattered light by pulse chirping, Phys. Rev. Accel. Beams **16**, 030705 (2013).

[23] B. Terzić, K. Deitrick, A. S. Hofler, and G. A. Krafft, Narrow-band Emission in Thomson Sources Operating in the High-Field Regime, Phys. Rev. Lett. **112**, 074801 (2014).

[24] S. G. Rykovanov, C. G. R. Geddes, C. B. Schroeder, E. Esarey, and W. P. Leemans, Reply to "comment on

'controlling the spectral shape of nonlinear thomson scattering with proper laser chirping", Phys. Rev. Accel. Beams **19**, 098002 (2016).

[25] C. Maroli, V. Petrillo, I. Drebot, L. Serafini, B. Terzić, and G. A. Krafft, Compensation of non-linear bandwidth broadening by laser chirping in Thomson sources, J. Appl. Phys. **124**, 063105 (2018).

[26] T. Heinzl, D. Seipt, and B. Kämpfer, Beam-shape effects in nonlinear Compton and Thomson scattering, Phys. Rev. A **81**, 022125 (2010).

[27] B. Terzić, A. Brown, I. Drebot, T. Hagerman, E. Johnson, G. A. Krafft, C. Maroli, V. Petrillo, and M. Ruijter, Improving performance of inverse Compton sources through laser chirping, Europhys. Lett. **126**, 12003 (2019).

[28] T. Xu, M. Chen, F.-Yu. Li, L.-L. Yu, Z.-M. Sheng, and J. Zhang, Spectrum bandwidth narrowing of Thomson scattering x-rays with energy chirped electron beams from laser wakefield acceleration, Appl. Phys. Lett. **104**, 013903 (2014).

[29] Z. Huang, Y. Ding, and C. B. Schroeder, Compact X-ray Free-Electron Laser from a Laser-Plasma Accelerator Using a Transverse-Gradient Undulator, Phys. Rev. Lett. **109**, 204801 (2012).

[30] R. Rossmanith, R. Aßmann, A. Bernhard, U. Dorda, B. Marchetti, V. Saile, P. Wesolowski *et al.*, A novel optical beam concept for producing coherent synchrotron radiation with large energy spread beams, Proc. of International Particle Accelerator Conference (IPAC'17), Copenhagen, Denmark (JACoW, Geneva, Switzerland, 2017), pp. 2646–2649, https://doi.org/10.18429/JACoW-IPAC2017-WEPAB032.

[31] T. Liu, T. Zhang, D. Wang, and Z. Huang, Compact beam transport system for free-electron lasers driven by a laser plasma accelerator, Phys. Rev. Accel. Beams **20**, 020701 (2017).

[32] J. D. Jackson, *Classical Electrodynamics*, 3rd ed. (John Wiley & Sons, New York, 1999).

[33] A. Di Piazza, Analytical infrared limit of nonlinear Thomson scattering including radiation reaction, arXiv: 1804.01160.

[34] E. S. Sarachik and G. T. Schappert, Classical theory of the scattering of intense laser radiation by free electrons, Phys. Rev. D **1**, 2738 (1970).

[35] V. Yu. Kharin, D. Seipt, and S. G. Rykovanov, Temporal laser-pulse-shape effects in nonlinear Thomson scattering, Phys. Rev. A **93**, 063801 (2016).

[36] M. S. Hussein, M. P. Pato, and A. K. Kerman, Theory of free-wave acceleration, Phys. Rev. A **46**, 3562 (1992).

[37] F. V. Hartemann, A. L. Troha, N. C. Luhmann, and Z. Toffano, Spectral analysis of the nonlinear relativistic Doppler shift in ultrahigh intensity Compton scattering, Phys. Rev. E **54**, 2956 (1996).

[38] D. Seipt, V. Kharin, S. Rykovanov, A. Surzhykov, and S. Fritzsche, Analytical results for nonlinear Compton scattering in short intense laser pulses, J. Plasma Phys. **82**, 655820203 (2016).

[39] M. Ruijter, V. Yu. Kharin, and S. G. Rykovanov, Analytical solutions for nonlinear Thomson scattering including radiation reaction, J. Phys. B **51**, 225701 (2018).

[40] C. Rödel, M. Heyer, M. Behmke, M. Kübel, O. Jäckel, W. Ziegler, D. Ehrt, M. C. Kaluza, and G. G. Paulus, High repetition rate plasma mirror for temporal contrast enhancement of terawatt femtosecond laser pulses by three orders of magnitude, Appl. Phys. B **103**, :295 (2011).

[41] A. Jeandet, A. Borot, K. Nakamura, S. W. Jolly, A. J. Gonsalves, C. Tóth, H.-S. Mao, W. P. Leemans, and F. Quéré, Spatio-temporal structure of a petawatt femtosecond laser beam, J. Phys. Photon. **1**, 035001 (2019).

[42] S. W. Botchway, P. Reynolds, A. W. Parker, and P. O'Neill, Chapter one - Laser-Induced radiation microbeam technology and simultaneous real-time fluorescence imaging in live cells, in *Imaging and Spectroscopic Analysis of Living Cells*, edited by P. Michael conn, Methods in Enzymology Vol. 504 (Academic Press, New York, 2012), pp. 3–28, https://doi.org/10.1016/B978-0-12-391857-4.00001-X.

[43] D. Seipt, S. G. Rykovanov, A. Surzhykov, and S. Fritzsche, Narrowband inverse Compton scattering x-ray sources at high laser intensities, Phys. Rev. A **91**, 033402 (2015).